Physics Letters B 752 (2016) 102–107

Contents lists available at ScienceDirect

Physics Letters B

www.elsevier.com/locate/physletb

# The pygmy quadrupole resonance and neutron-skin modes in $^{124}$Sn

M. Spieker [a,*], N. Tsoneva [b,c,d], V. Derya [a], J. Endres [a], D. Savran [e,b], M.N. Harakeh [f], S. Harissopulos [g], R.-D. Herzberg [h], A. Lagoyannis [g], H. Lenske [c], N. Pietralla [i], L. Popescu [f,j], M. Scheck [k,i], F. Schlüter [a], K. Sonnabend [l], V.I. Stoica [f,1], H.J. Wörtche [f,1], A. Zilges [a]

[a] Institut für Kernphysik, Universität zu Köln, Zülpicher Straße 77, D-50937 Köln, Germany
[b] Frankfurt Institute for Advanced Studies, D-60438 Frankfurt am Main, Germany
[c] Institut für Theoretische Physik, Universität Gießen, Heinrich-Buff-Ring 16, D-35392 Gießen, Germany
[d] Institute for Nuclear Research and Nuclear Energy, 1784 Sofia, Bulgaria
[e] ExtreMe Matter Institute EMMI and Research Division, GSI Helmholtzzentrum für Schwerionenforschung GmbH, D-64291 Darmstadt, Germany
[f] KVI-CART, University of Groningen, 9747 AA Groningen, The Netherlands
[g] Institute for Nuclear Physics, N.C.S.R. Demokritos Athens, GR-15310 Athens, Greece
[h] Oliver Lodge Laboratory, University of Liverpool, Liverpool L69 7ZE, United Kingdom
[i] Institut für Kernphysik, TU Darmstadt, D-64289 Darmstadt, Germany
[j] Belgian Nuclear Research Centre SCK*CEN, B-2400 Mol, Belgium
[k] University of the West of Scotland, Paisley PA1 2BE, United Kingdom
[l] Institut für Angewandte Physik, Goethe-Universität Frankfurt am Main, 60438 Frankfurt am Main, Germany

ARTICLE INFO

*Article history:*
Received 28 July 2015
Received in revised form 20 October 2015
Accepted 3 November 2015
Available online 10 November 2015
Editor: V. Metag

*Keywords:*
Atomic nuclei
Collective quadrupole excitations
Pygmy quadrupole resonance
$^{124}$Sn

ABSTRACT

We present an extensive experimental study of the recently predicted pygmy quadrupole resonance (PQR) in Sn isotopes, where complementary probes were used. In this study, $(\alpha,\alpha'\gamma)$ and $(\gamma,\gamma')$ experiments were performed on $^{124}$Sn. In both reactions, $J^\pi = 2^+$ states below an excitation energy of 5 MeV were populated. The $E2$ strength integrated over the full transition densities could be extracted from the $(\gamma,\gamma')$ experiment, while the $(\alpha,\alpha'\gamma)$ experiment at the chosen kinematics strongly favors the excitation of surface modes because of the strong $\alpha$-particle absorption in the nuclear interior. The excitation of such modes is in accordance with the quadrupole-type oscillation of the neutron skin predicted by a microscopic approach based on self-consistent density functional theory and the quasiparticle-phonon model (QPM). The newly determined $\gamma$-decay branching ratios hint at a non-statistical character of the $E2$ strength, as it has also been recently pointed out for the case of the pygmy dipole resonance (PDR). This allows us to distinguish between PQR-type and multiphonon excitations and, consequently, supports the recent first experimental indications of a PQR in $^{124}$Sn.



The atomic nucleus is a strongly coupled system consisting of nucleons, namely the protons and neutrons. This mesoscopic system is known to exhibit collective excitations of different multipolarities due to the strong interaction between the individual constituents. Among these excitations, the isovector giant dipole resonance (IVGDR) and the isoscalar giant quadrupole resonance (ISGQR) have been systematically studied and their properties have been well determined, see, e.g., Ref. [1]. These very collective excitations are typically found above the particle-emission threshold. In recent years, the nuclear multipole response below and just above the particle-emission threshold has attracted a lot of interest. In particular, the experimental observation of a pygmy dipole resonance (PDR) triggered systematic experimental and theoretical studies, see the review articles [2–4]. Many microscopic models suggest that the experimentally found PDR can be identified with an oscillation of a neutron skin against an isospin-saturated proton–neutron core [5–11]. While the existence of the neutron skin in heavy nuclei has been experimentally established [12–17], it is not evident that the PDR would be a neutron-skin excitation mode. To address this question, the $(\alpha,\alpha'\gamma)$ experiments provided important insights [18,19]. An isospin splitting of the low-lying electric dipole strength was observed, in which a class of $J^\pi = 1^-$ states was found, which could be identified with a more isoscalar surface mode in contrast to the isovector $E1$ strength measured in $(\gamma,\gamma')$ experiments [19,20]. These results were independently

* Corresponding author.
*E-mail address:* spieker@ikp.uni-koeln.de (M. Spieker).
[1] Present address: INCAS[3], Dr. Nassaulaan 9, 9401 AJ Assen, The Netherlands.

http://dx.doi.org/10.1016/j.physletb.2015.11.004

confirmed by using the $(^{17}O, ^{17}O')$ reaction [21,22]. Also in these experimental studies, the scattered ions were detected in coincidence with the de-exciting $\gamma$ rays [3]. For the $\gamma$-ray detection the powerful AGATA demonstrator array had been used. Another important approach to verify the unique character of the PDR has been the recent study of the $\gamma$-decay behavior of the $1^-$ states in $^{60}$Ni [23], $^{94}$Mo [24], $^{130}$Te [25], $^{140}$Ce [26], and $^{142}$Nd [27]. It could be shown that the PDR does not decay according to the statistical model but, instead, is strongly coupled to the ground state. These experimental findings establish the PDR as a unique mode, and if its connection to the neutron-skin oscillation predicted by different theoretical approaches is indeed true, its implications are manifold not just from a nuclear structure perspective. For instance, some theoretical work claims that PDR studies and the nuclear $E1$ strength in general can provide important constraints on the nuclear equation of state (EOS) by probing the neutron skin, see, e.g., [14,28–30]. Corresponding constraints would help to improve the description of neutron stars [29,31–34]. However, other theories question the strong correlation between the low-lying $E1$ strength and certain parameters of the equation of state, see, e.g., Ref. [35]. Certainly, the general existence of additional dipole strength below and close to the particle-emission threshold does have an impact on the nucleosynthesis processes [36–40]. It is evident that more experimental data are needed to unambiguously identify an effect of the neutron skin on excited states of the atomic nucleus. One way to extend the experimental studies of the neutron skin has been recently proposed in the framework of a microscopic theoretical model incorporating self-consistent energy-density functional (EDF) theory and the quasiparticle-phonon model (QPM) [41]. Here, it was shown that the presence of the neutron skin should not only affect dipole excitations but also excitations of higher multipolarity. In particular, a pygmy quadrupole resonance (PQR) was predicted [41].

First experimental indications of PQR states were very recently found in $^{124}$Sn using the $(^{17}O, ^{17}O')$ reaction [42]. In this work, the authors proved the electric quadrupole character of the transitions of interest and inferred a general isoscalar character of the quadrupole excitations [42]. However, multiphonon excitations are also expected to show a dominantly isoscalar character, which complicates a clear identification of PQR states on the basis of inelastic scattering with surface-dominant isoscalar probes in contrast to the PDR case.

It is therefore the purpose of this letter to present the missing experimental information on $E2$ strength up to 5 MeV and to establish the $\gamma$-decay behavior of $2^+$ states as a clear signature to distinguish PQR-type and multiphonon states. Furthermore, a stringent comparison to theory is used to address the possibility of the existence of a PQR due to neutron-skin oscillations [41,42].

We have performed, as in the case of the PDR, two complementary experiments, namely an $(\alpha, \alpha'\gamma)$ experiment and a $(\gamma, \gamma')$ experiment. We keep the description of the experimental setups and analysis procedures brief, since these have already been described at length in our work concerning the PDR in $^{94}$Mo [43], $^{124}$Sn [44], $^{138}$Ba and $^{140}$Ce [45], and the $N = 82$ isotones [46].

The $(\alpha, \alpha'\gamma)$ experiment was performed using the Big-Bite Spectrometer (BBS) at the Kernfysisch Versneller Instituut in Groningen, the Netherlands. Here, $\alpha$ particles with an energy of $E_\alpha = 34$ MeV/u were provided by the AGOR cyclotron and impinged onto a highly enriched 7 mg/cm$^2$ $^{124}$Sn target. The inelastically scattered $\alpha$ particles were detected by the EUROSUPERNOVA detection system after being bent through the BBS. To detect the inelastically scattered $\alpha$ particles, which are sensitive to isoscalar excitations in the entrance channel, in coincidence with the de-exciting $\gamma$ rays, an array of six HPGe detectors was positioned around the target chamber. This combined setup allowed for a selective state-by-state analysis due to the high energy resolution of the HPGe detectors [47]. By setting gates in the $\alpha\gamma$-coincidence matrix, we were also able to study $\gamma$ decays leading to different final states and, thus, to determine $\gamma$-decay branching ratios. For any given excited state the $\gamma$-decay ratio, i.e. the $\gamma$-decay intensity to any considered final state relative to, e.g., the decay intensity to the ground state could be determined as follows:

$$\frac{\Gamma_i}{\Gamma_{0_1^+}} = \frac{A_i}{A_{0_1^+}} \frac{\sum_{j=1}^{16} \epsilon_{abs,j}(E_{\gamma_{0_1^+}})\, \Delta_{live,j}\, W_{0_1^+,j}(\Omega_\gamma)}{\sum_{i=1}^{16} \epsilon_{abs,j}(E_{\gamma_i})\, \Delta_{live,j}\, W_{i,j}(\Omega_\gamma)}. \quad (1)$$

In Eq. (1), $i$ denotes the specifically selected final state and $j$ enumerates the individual HPGe detectors. Furthermore, $A_i$ is the integrated peak area for the $\gamma$ transition of interest, $\epsilon_{abs,j}(E_{\gamma_i})$ is the absolute detector efficiency, $\Delta_{live,j}$ is the relative live time of the HPGe detector, and $W_{i,j}(\Omega_\gamma)$ resembles the $\alpha\gamma$-angular correlation, which will be discussed in more detail below. For a more complete description of the different quantities, see Ref. [44]. The final ground-state $\gamma$-decay branching ratio $\Gamma_0/\Gamma$ can be determined by taking into account all observed branching decays. The present data allowed us to study $\gamma$ decays leading to final states up to the $2_3^+$ state of $^{124}$Sn. To illustrate the importance of this $\gamma$-decay branching and its determination, Fig. 1 shows the $\gamma$-ray spectrum of excited states decaying directly to the ground state of $^{124}$Sn as well as a $\gamma$-ray spectrum of states, which decay to the first $2^+$ state. The PDR and $2^+$ states of a possible PQR are marked.

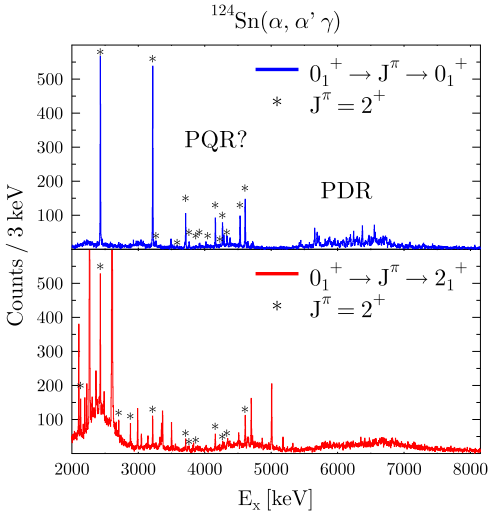


**Fig. 1.** (Color online.) $\gamma$-ray spectra resulting from ground-state transitions (blue spectrum in top panel) and transitions to the $2_1^+$ state (red spectrum in bottom panel) of states excited in the $^{124}$Sn$(\alpha, \alpha')$ reaction. $J^\pi = 2^+$ states of a possible PQR are marked with asterisks. For completeness, the energy region of the PDR is also shown. Note that the excitation energy $E_x$ is given instead of the $\gamma$-ray energy $E_\gamma$ to identify $\gamma$-decay branching.

As mentioned above, the combined setup enabled us to measure $\alpha\gamma$-angular correlations [44]. These confirmed the quadrupole character of our transitions of interest below 5 MeV by comparing with predictions from combined DWBA calculations with CHUCK3 [48] yielding scattering amplitudes and ANGCOR [49] calculations using these scattering amplitudes to generate the angular correlations; see Fig. 2. These results are in agreement with the previous results of Ref. [42].

The second experiment was performed at the S-DALINAC in Darmstadt using the DHIPS setup [50]. Here, we bombarded a highly enriched, 1.8 g thick $^{124}$Sn target with bremsstrahlung resulting from incident electrons of $E_{e^-} = 7.8$ MeV. These nuclear resonance fluorescence (NRF) [51] data allowed for the determination of previously unknown B(E2)↑ values for a group of states

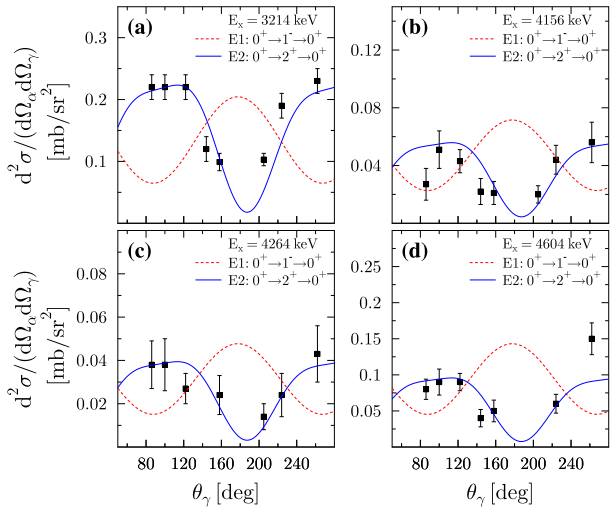


**Fig. 2.** (Color online.) Experimental double-differential cross sections for four different $J^\pi = 2^+$ states in $^{124}$Sn (black squares with error bars) as well as theoretical averaged angular correlations for dipole (red dashed lines) and quadrupole (blue solid lines) transitions as explained in Ref. [44]. For examples of experimental dipole transitions we refer the reader to Ref. [44].

above 4 MeV. However, since the electron energy was chosen to also study the PDR, feeding of $J^\pi = 2^+$ states could not be excluded and, therefore, it needs to be corrected. The observable in NRF experiments is $\Gamma_0^2/\Gamma$ [51], where $\Gamma_0$ is the ground-state width and $\Gamma$ the total width. Ref. [52] proposed that one could extract an effective feeding width $\Gamma_{\text{feed}}$, resulting from inelastic transitions to higher-lying states followed by $\gamma$-decay to the level of interest, to correct for feeding effects, when assuming $\Gamma_0 \cdot (\Gamma_0 + \Gamma_{\text{feed}})/\Gamma$. The real ground-state width $\Gamma_0$ of five $2^+$ states below 4 MeV in $^{124}$Sn had been previously determined with different probes [53], including NRF experiments with an electron energy below 4 MeV [54]. Our newly determined and previously known ground-state $\gamma$-decay branching ratios $\Gamma_0/\Gamma$ as well as our NRF data on $^{124}$Sn, obtained with higher electron energies, allowed us to study feeding effects. We found that a constant effective feeding width of $\Gamma_{\text{feed}} = 9(2)$ meV does describe the NRF data, see Fig. 3, better than when assuming an energy-dependent feeding as proposed in Ref. [52]. Note that the quantity $\Gamma_{\text{feed}}$ can be directly obtained from the experimental data when the real $\Gamma_0$ is known [52]. This result, see Fig. 3, enabled us to correct our newly measured $E2$ strength without using any theoretically predicted statistical $\gamma$-decay behavior.

The combined results of both experiments and the measured B(E2)↑ values from Refs. [53,54] are shown in Fig. 4. To determine the $\alpha$-scattering cross sections (Fig. 4(a)), the isoscalar $B(E2)_{IS}$ ↑ values (Fig. 4(b)), and the B(E2)↑ values (Fig. 4(c)), the mostly newly measured $\gamma$-decay branching ratios of our $(\alpha,\alpha'\gamma)$ experiment have been used. The ground-state $\gamma$-decay branching ratio $b_0$, i.e. $\Gamma_0/\Gamma$, is shown in Fig. 4(d). The isoscalar $B(E2)_{IS}$ ↑ values were calculated from the $\alpha$-scattering cross sections using the coupled-channels program CHUCK3 with a standard collective form factor [48] and the program code BEL [55] with implicit folding procedure. In both cases, the global optical potential from Ref. [56] was used. Coulomb excitation (Coulex) was explicitly included in the inelastic scattering process [48] since Coulex can take place even at larger distances beyond the nuclear radius for collective quadrupole excitations. The concrete procedure of extracting reduced transition strengths from scattering cross sections has been outlined in, e.g., Refs. [1,57].

Four new B(E2)↑ values above 4 MeV could be determined in our NRF experiment, see Fig. 4(c). Note that these values have been

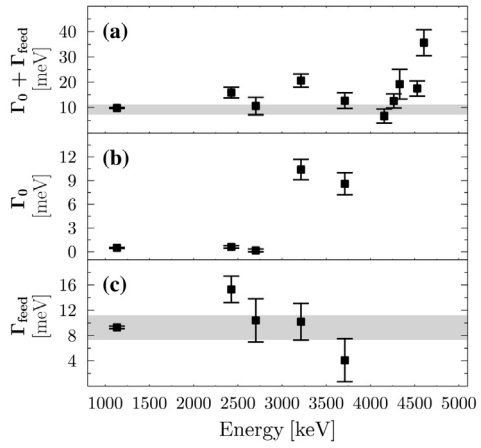


**Fig. 3.** (Color online.) (a) $\Gamma_0 + \Gamma_{\text{feed}}$ obtained from the present NRF experiment for the observed $2^+$ states in $^{124}$Sn. (b) Unfed $\Gamma_0$ taken from [53,54]. (c) Effective feeding width $\Gamma_{\text{feed}}$ determined in this work. In panels (a) and (c), the mean effective feeding width 9(2) meV is also shown in grey.

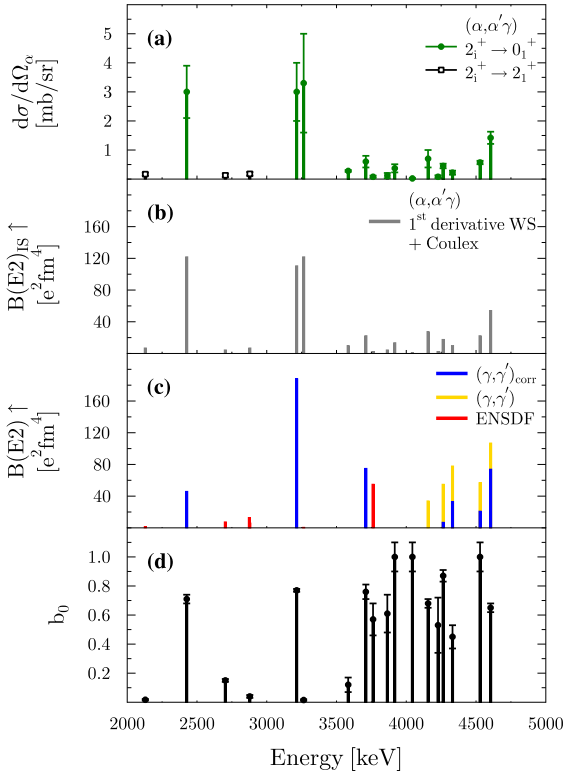


**Fig. 4.** (Color online.) (a) $\alpha$-scattering cross sections. States decaying to the ground state are shown in green. States, which have not been observed to decay to the ground state but to the $2_1^+$ state are shown in black. (b) $B(E2)_{IS}$ ↑ values deduced from the $\alpha$-scattering cross sections, see text. (c) B(E2)↑ values from NRF measurements in blue. Values below 4 MeV are adopted from Ref. [54]. The feeding-corrected values above 4 MeV have been determined in this work. For completeness, the uncorrected values are also presented in yellow. In red, additionally adopted values from Ref. [53] are shown. (d) Ground-state $\gamma$-decay branching ratio $b_0 = \Gamma_0/\Gamma$.

corrected for feeding and, thus, represent more likely lower than upper limits since our feeding correction has been conservative. Furthermore, additional $\gamma$-decay channels, which have not been observed previously or in our work could alter the ground-state $E2$ strength. For completeness also the uncorrected B(E2)↑ values are shown in Fig. 4(c). Keeping these experimental uncertainties in mind, it is a striking experimental observation that all $J^\pi = 2^+$ states above $E_x = 3.5$ MeV as well as two states below this exci-

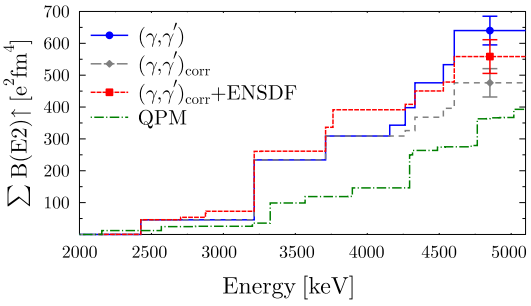


**Fig. 5.** (Color online.) Running sum of the $E2$ strength. Shown are the uncorrected data (solid blue line/blue circle with error bar), the feeding-corrected data (dashed grey line/grey diamond with error bar), the feeding-corrected data combined with additional data from ENSDF [53] (dashed red line/red square with error bar), and the QPM predictions (dash-dotted green line).

tation energy show a quite large $b_0$; see Fig. 4(d), and as such are not likely candidates for pure quadrupole-multiphonon excitations. In fact, such candidates could be identified with, e.g., small $\alpha$ cross sections when gating on transitions to the $2_1^+$ state; see the black symbols in Fig. 4(a), and corresponding small $b_0$ values (Fig. 4(d)). These states are found at lower excitation energies, see, e.g., Ref. [58]. In general, there are more $2^+$ states that have been observed with the $\alpha$ than with the photon probe, which might hint at a small ground-state width $\Gamma_0$, even though the ground-state decay channel is dominant. It should be stressed that the NRF experiments include isovector (IV) and isoscalar (IS) contributions to the B(E2) value, while the $\alpha$ particles only probe the isoscalar part of the transition matrix element. The independently measured values in both experiments allow to recognize dominant isoscalar character of the $E2$ excitations in agreement with Ref. [42]. In other cases, IV and IS contributions might interfere destructively or constructively and, thus, change the picture of the total $E2$ strength in comparison to the isoscalar $E2$ strength. It has already been suggested that the true nature of neutron-skin excitations and their collectivity might not be fully accessed by the strength distribution probed with electromagnetic probes only. Of course, these data yield very valuable information when comparing with other probes and serve as a benchmark for theoretical models. However, in the case of the quadrupole states we also need another observable to identify possible PQR character. In the present kinematics the $(\alpha, \alpha')$ reaction is sensitive to nuclear excitations with surface-dominant transition densities. Furthermore, the $\gamma$-decay behavior, also probed in our $(\alpha, \alpha'\gamma)$ experiment, might provide a clearer signature since, as mentioned above, a group of states shows a decay behavior, i.e. $b_0 \geq 0.5$, very different from that expected from multiphonon excitations.

In the following, we will compare the new and available experimental data with quasiparticle random-phase approximation (QRPA) and QPM calculations. We want to emphasize that the present QRPA and QPM calculations have been performed with model parameters from Ref. [41] which have been used to predict the PQR. Further details of the model can also be found in [6,41]. First, we compare the running sum of the $E2$ strength in Fig. 5. As can be seen, the QPM predicts a higher fragmentation of the $E2$ strength but agrees with the $(\gamma, \gamma')$ total strength up to 5 MeV after this has been corrected for feeding as described above. However, from our $(\alpha, \alpha'\gamma)$ experiment we know that there are more $2^+$ states which are strongly coupled to the ground state, see Fig. 4(d), and their strength and the strength of weaker and also less strongly coupled states might have been missed in $(\gamma, \gamma')$. We therefore also considered adopted $E2$ strength from [53]. Within the experimental uncertainties the agreement for the total strength is still good, and the experimental fragmentation is

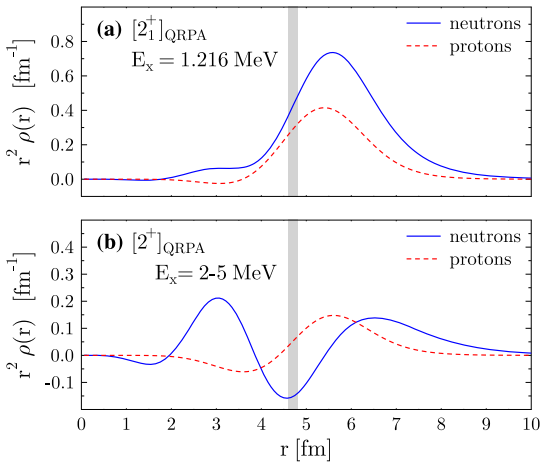


**Fig. 6.** (Color online.) (a) Transition density of the $[2_1^+]_{\mathrm{QRPA}}$ state at 1.216 MeV and (b) summed transition density for the $[2^+]_{\mathrm{QRPA}}$ states between 2 MeV and 5 MeV in $^{124}$Sn. The neutron-skin thickness of 0.18 fm is indicated in grey.

indeed enhanced in agreement with theory and the experimental isoscalar $E2$ strength. As has been shown in Ref. [41], the low-lying $E2$ strength from the PQR region, $E_x = 2$–5 MeV in Sn isotopes, mainly originates from a sequence of QRPA states with almost pure neutron structure related to excitations of weakly bound neutron two-quasiparticle (2QP) states from the Fermi surface. The collectivity of the PQR QRPA states increases with excitation energy. In particular, the lowest-lying $[2_2^+]_{\mathrm{QRPA}}$ and $[2_3^+]_{\mathrm{QRPA}}$ states are non-collective and the main contribution to their state vectors is related to more than 80% to a single neutron 2QP component, i.e. 87.3% $\left(2d_{3/2} \otimes 2d_{3/2}\right)_\nu$ and 82.9% $\left(3s_{1/2} \otimes 2d_{3/2}\right)_\nu$ in $^{124}$Sn, respectively. This situation changes for the QRPA states above 3 MeV where several neutron 2QP components contribute, e.g., $\left(1g_{7/2} \otimes 2d_{3/2}\right)_\nu$, $\left(2d_{5/2} \otimes 2d_{3/2}\right)_\nu$, $\left(1g_{7/2} \otimes 1g_{7/2}\right)_\nu$, and $\left(2d_{5/2} \otimes 3s_{1/2}\right)_\nu$ in addition to the aforementioned components.

The different characters of the low-energy $2^+$ states can also be inferred in the case of $^{124}$Sn from the transition densities; see Fig. 6. While the $[2_1^+]_{\mathrm{QRPA}}$ state corresponds to an almost pure isoscalar oscillation of both protons and neutrons at the nuclear surface and can be identified with the experimental $2_1^+$ state, the summed transition density of QRPA $2^+$ states between 2 MeV and 5 MeV is dominated by neutron oscillations at the nuclear surface. This corresponds to the quadrupole-type oscillation of the neutron skin. The transition densities between 2 MeV and 5 MeV additionally exhibit IV character. This observation could explain the interference pattern of IV and IS parts, which might have been observed experimentally, even though a dominantly isoscalar character has been inferred in Refs. [41,42]; see Figs. 4(b) and (c). However, it has to be stressed that previous studies using the $(^{17}\mathrm{O}, ^{17}\mathrm{O}')$ reaction pointed out that in contrast to $1^-$ states of the PDR region, where neutron-dominated transition densities at the surface had to be used to obtain agreement with the experimental data, the $2^+$ states could be described well with a standard collective form factor, see, e.g., Refs. [3,21,22,42,59]. In fact, this might be expected when comparing Figs. 6(a) and (b) considering that the difference of the neutron-skin effect is not as pronounced as in the PDR case when comparing with almost pure isoscalar quadrupole-surface vibrations. This could result in similar and, thus, currently indistinguishable form factors at the nuclear surface, see, e.g., Ref. [59].

Therefore, in order to obtain a clearer picture and to test the PQR wave functions further, we compare the theoretical and experimental ground-state $\gamma$-decay branching ratio $b_0$. To put this comparison on fair ground, we limited the final states considered in the QPM calculation of $b_0$ to the final states, which were ac-

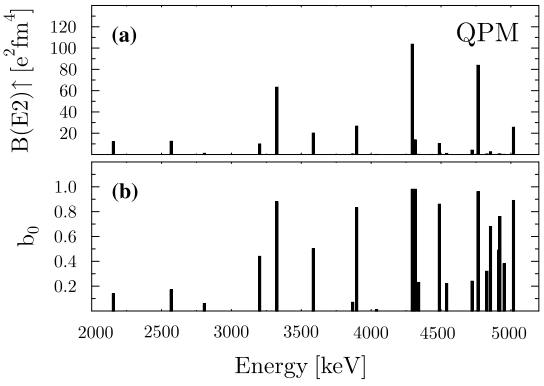


**Fig. 7.** (a) $E2$ strength above 2 MeV and below 5 MeV as well as (b) the ground-state $\gamma$-decay branching ratio $b_0$ predicted by the QPM.

cessible in our experiment. These were final states up to the $2_3^+$ state. The QPM results are shown in Fig. 7. As in our experiment, we do observe a predominant decay of $2^+$ states above 3 MeV to the ground state; see Fig. 7(b). In fact, the general trend is in remarkable accordance with the experimental observations, displayed in Fig. 4(d). This can be explained by investigating the fragmentation pattern of the PQR QRPA $2^+$ states over the excited $2^+$ states obtained from the QPM calculations. The theoretical analysis shows that the QPM $2^+$ states from the PQR region have a quite complex structure, which is a mixture of one-, two-, and even three-phonon components. However, the most collective component is the one-phonon component related to the PQR $[2_4^+]_{\mathrm{QRPA}}$, $[2_5^+]_{\mathrm{QRPA}}$, and $[2_6^+]_{\mathrm{QRPA}}$ states, which is a substantial part of all QPM $2^+$ wave functions above 3 MeV. This collective admixture explains the large $b_0$ values and supports large $b_0$ values to be a possible experimental signature for PQR states. The exhaustion of the quadrupole ISEWSR, see, e.g., [1,60], when identifying PQR states with $b_0 \geq 0.5$ amounts to 3.8(5)% for the $(\alpha, \alpha')$ data and to 5.5(6)% (7.3(6)% without feeding correction) for the NRF and ENSDF data, which however also contain IV contributions. The exhaustion of the ISEWSR in the QPM amounts to 4.1% for the PQR states. These values differ from the value of 13.6% reported in Ref. [42], where all $E2$ strength below 5 MeV, including the $B(E2; 0_1^+ \rightarrow 2_1^+)$ strength, was considered. We want to note explicitly, that both experimental values are consistent with the exhaustion of the dipole ISEWSR in the case of the PDR in $^{124}$Sn, which was reported to be 2.2(3)% for strength accumulated in discrete peaks and 7.8(7)% if unresolved strength was taken into account [22]. We also want to emphasize that the neutron-skin thickness of 0.18 fm predicted by the present model appears to be in nice agreement with the value of 0.148(34) fm found in Ref. [61] by means of the dipole polarizability of $^{120}$Sn.

In conclusion, we have presented new experimental data on quadrupole excitations below 5 MeV, which came from two complementary experiments, which indicate the existence of a PQR in $^{124}$Sn and which support the recent conclusions [42]. From the $(\alpha, \alpha'\gamma)$ experiment we have, in addition to the $\alpha$ scattering cross sections, extracted the isoscalar $E2$ strength and ground-state $\gamma$-decay branching ratios. The latter has subsequently been used to correct the $E2$ strength measured in our $(\gamma, \gamma')$ experiment above 4 MeV. The new data allow for a stringent comparison between experiment and theory. The QPM reproduces the experimental summed $E2$ strength up to 5 MeV and predicts it to be due to a quadrupole surface oscillation of a neutron skin. This prediction was further tested by means of the ground-state $\gamma$-decay branching ratio, which was accessed theoretically and experimentally. The general agreement is good and the ground-state $\gamma$-decay ratio $b_0$ may be used to identify possible PQR states. Our work thus provides additional evidence for a new kind of excitation mode, namely the PQR, which is due to a quadrupole-type oscillation of the neutron skin. This result further supports the existence of the neutron skin, and gives new input as to whether the neutron skin does affect nuclear excitations and to whether the PDR is partly generated by dipole-type neutron-skin oscillations. To further test these and previous conclusions, systematic $(\alpha, \alpha'\gamma)$, $(p, p'\gamma)$, $(^{17}\mathrm{O}, ^{17}\mathrm{O}'\gamma)$, and $(\gamma, \gamma')$ studies of quadrupole excitations in the Sn and other isotopes are highly desirable. Furthermore, also the feeding contributions, discussed in this letter, should be studied using, e.g., the $\gamma^3$ setup at HI$\gamma$S [62] or the opportunities at the future ELI-NP facility in Bucharest (Romania) [63]. The neutron-skin thickness of $^{124}$Sn could be further constrained measuring, e.g., the dipole polarizability at RCNP, Osaka (Japan).

## Acknowledgements

This work was supported by the Deutsche Forschungsgemeinschaft (ZI 510/7-1 and SFB 634), by the LOEWE program of the State of Hesse (Helmholtz International Center for FAIR), and by the Alliance Program of the Helmholtz Association (HA216/EMMI). The research has been further supported by the EU under EURONS Contract No. RII3-CT-2004-506065 in the 6th framework program, by the DFG cluster of excellence Origin and Structure of the Universe, by the Russian Federal Education Agency Program, and by UK STFC. N.T. is also supported by BMBF grant 05P12RGFTE. M.S. is supported by the Bonn-Cologne Graduate School of Physics and Astronomy.

## References

[1] M.N. Harakeh, A. van der Woude, Giant Resonances, Oxford University Press, New York, 2001.
[2] D. Savran, T. Aumann, A. Zilges, Experimental studies of the pygmy dipole resonance, Prog. Part. Nucl. Phys. 70 (2013) 210.
[3] A. Bracco, F.C.L. Crespi, E.G. Lanza, Eur. Phys. J. A 51 (2015) 99.
[4] N. Paar, D. Vretenar, E. Khan, Rep. Prog. Phys. 70 (2007) 691.
[5] N. Tsoneva, H. Lenske, C. Stoyanov, Phys. Lett. B 586 (2004) 213.
[6] N. Tsoneva, H. Lenske, Phys. Rev. C 77 (2008) 024321.
[7] E. Litvinova, P. Ring, V. Tselyaev, K. Langanke, Phys. Rev. C 79 (2009) 054312.
[8] E.G. Lanza, et al., Phys. Rev. C 84 (2011) 064602.
[9] T. Inakura, T. Nakatsukasa, K. Yabana, Phys. Rev. C 84 (2011) 021302(R).
[10] E. Yüksel, E. Khan, K. Bozkurt, Nucl. Phys. A 877 (2012) 35.
[11] V. Baran, et al., Phys. Rev. C 88 (2013) 044610.
[12] A. Krasznahorkay, et al., Phys. Rev. Lett. 66 (1991) 1287.
[13] A. Krasznahorkay, et al., Phys. Rev. Lett. 82 (1999) 3216.
[14] A. Tamii, et al., Phys. Rev. Lett. 107 (2011) 062502.
[15] S. Abrahamyan, et al., Phys. Rev. Lett. 108 (2012) 112502.
[16] A. Krasznahorkay, N. Paar, D. Vretenar, M.N. Harakeh, Phys. Lett. B 720 (2013) 428.
[17] C.M. Tarbert, et al., Phys. Rev. Lett. 112 (2014) 242502.
[18] D. Savran, et al., Phys. Rev. Lett. 97 (2006) 172502.
[19] J. Endres, et al., Phys. Rev. Lett. 105 (2010) 212503.
[20] E.G. Lanza, A. Vitturi, E. Litvinova, D. Savran, Phys. Rev. C 89 (2014) 041601(R).
[21] F.C.L. Crespi, et al., Phys. Rev. Lett. 113 (2014) 012501.
[22] L. Pellegri, et al., Phys. Lett. B 738 (2014) 519.
[23] M. Scheck, et al., Phys. Rev. C 87 (2013) 051304(R).
[24] C. Romig, et al., Phys. Rev. C 88 (2013) 044331.
[25] J. Isaak, et al., Phys. Lett. B 727 (2013) 361.
[26] C. Romig, et al., Phys. Lett. B 744 (2015) 369.
[27] C.T. Angell, et al., Phys. Rev. C 86 (2012) 051302(R); C.T. Angell, et al., Phys. Rev. C 91 (2015) 039901(E).
[28] A. Klimkiewicz, et al., Phys. Rev. C 76 (2007) 051603.
[29] B.-A. Li, A. Ramos, G. Verde, I. Vidaña, Eur. Phys. J. A 50 (2014).
[30] J. Piekarewicz, Phys. Rev. C 83 (2011) 034319.
[31] C.J. Horowitz, J. Piekarewicz, Phys. Rev. Lett. 86 (2001) 5647.
[32] J. Piekarewicz, et al., Phys. Rev. C 85 (2012) 041302(R).
[33] F.J. Fattoyev, J. Piekarewicz, Phys. Rev. C 86 (2012) 015802.
[34] B. Alex Brown, A. Schwenk, Phys. Rev. C 89 (2014) 011307(R).
[35] P.-G. Reinhard, W. Nazarewicz, Phys. Rev. C 87 (2013) 014324.
[36] S. Goriely, E. Khan, M. Samyn, Nucl. Phys. A 739 (2004) 331.

[37] E. Litvinova, N. Belov, Phys. Rev. C 88 (2013) 031302(R).
[38] B.V. Kheswa, et al., Phys. Lett. B 744 (2015) 268.
[39] N. Tsoneva, S. Goriely, H. Lenske, R. Schwengner, Phys. Rev. C 91 (2015) 044318.
[40] L. Netterdon, et al., Phys. Lett. B 744 (2015) 358.
[41] N. Tsoneva, H. Lenske, Phys. Lett. B 695 (2011) 174.
[42] L. Pellegri, et al., Phys. Rev. C 92 (2015) 014330.
[43] V. Derya, et al., Nucl. Phys. A 906 (2013) 94.
[44] J. Endres, et al., Phys. Rev. C 85 (2012) 064331.
[45] J. Endres, et al., Phys. Rev. C 80 (2009) 034302.
[46] D. Savran, et al., Phys. Rev. C 84 (2011) 024326.
[47] D. Savran, et al., Nucl. Instrum. Methods A 564 (2006) 267.
[48] P.D. Kunz, J.R. Comfort, Program CHUCK3 (1978) extended version (unpublished).
[49] M.N. Harakeh, L.W. Put, Program ANGCOR (1979) KVI internal report 67i (unpublished).
[50] K. Sonnabend, et al., Nucl. Instrum. Methods A 640 (2011) 6.
[51] U. Kneissl, H.H. Pitz, A. Zilges, Prog. Part. Nucl. Phys. 37 (1996) 349.
[52] K. Govaert, et al., Phys. Rev. C 57 (1998) 2229.
[53] ENSDF, NNDC online data service, ENSDF database, http://www.nndc.bnl.gov/ensdf/, 2015.
[54] J. Bryssinck, et al., Phys. Rev. C 61 (2000) 024309.
[55] M.N. Harakeh, Program BEL (1981) KVI internal report 77 (unpublished).
[56] M. Nolte, H. Machner, J. Bojowald, Phys. Rev. C 36 (1987) 1312.
[57] K. van der Borg, M.N. Harakeh, A. van der Woude, Nucl. Phys. A 365 (1981) 243.
[58] D. Bandyopadhyay, et al., Nucl. Phys. A 747 (2005) 206.
[59] F.C.L. Crespi, et al., Phys. Rev. C 91 (2015) 024323.
[60] J. Enders, O. Karg, P. von Neumann-Cosel, V.Yu Ponomarev, Eur. Phys. J. A 31 (2007) 15.
[61] T. Hashimoto, et al., Phys. Rev. C 92 (2015) 031305(R).
[62] B. Löher, et al., Nucl. Instrum. Methods Phys. Res. A 723 (2013) 136.
[63] C. Ur, et al., Nucl. Instrum. Methods Phys. Res. B 355 (2015) 198.